

ORTHOGONAL Projection Based Fully Constrained Spectral Unmixing

Meiping Song¹, Hsiao-Chi Li², Yao Li², Cheng Gao² and Chein-I Chang²

¹Information and Technology College, Dalian Maritime University
1 Linghai Road, Dalian, China

²Remote Sensing Signal and Image Processing Laboratory
Department of Computer Science and Electrical Engineering
University of Maryland, Baltimore County, Baltimore, MD 21250

ABSTRACT

OSP has been used widely in detection and abundance estimation for about twenty years. But it can't apply nonnegative and sum-to-one constraints when being used as an abundance estimator. Fully constrained least square algorithm does this well, but its time cost increases greatly as the number of endmembers grows. There are some tries for unmixing spectral under fully constraints from different aspects recently. Here in this paper, a new fully constrained unmixing algorithm is prompted based on orthogonal projection process, where a nearest projected point is defined onto the simplex constructed by endmembers. It is much easier, and it is faster than FCLS with the mostly same unmixing results. It is also compared with other two constrained unmixing algorithms, which shows its effectiveness too.

Keywords: Orthogonal projection, Fully constrained unmixing

1. Introduction

In recent years, hyperspectral image and its analysis technologies have received more and more focuses from the researchers in remote sensing field. The imagery collects much more data and information of the land cover with its high spectral resolution, widely applied in land cover classification, quantity analysis and target detection for agriculture and military purposes. Due to its low spatial resolution, there may contains several materials in one pixel. How to decompose the mixed pixel into a collection of constituent spectral signatures, called endmembers, and a set of corresponding fractions, called abundance, is an important topic in identifying individual materials and quantity analysis.

Linear spectral unmixing has been researched more than 20 years based on linear mixture model (LMM) and received great success. This model has a clear physical meaning and is convenient for implementation. Its unmixing process involves two steps, endmember extraction and abundance estimation. Endmember extraction can be accomplished by corresponding algorithms, such as automatic target generating process, N-FINDR, and iterative error analysis. Abundance estimation is often solved based on a least squares criterion. Usually, there are two more constraints to make the resulted abundance practical and meaningful. The first constraint is that abundances of all endmembers should sum to 1 (ASC). And the second one is that abundance of every endmember should be greater than 0, which means nonnegative (ANC). ASC is easy to meet, but the ANC is much hard because it can't get a close-form solution through an analytical way.

There have been many efforts devoted to solve the fully constrained least squares problems. Quadratic programming technique is used for the optimization process^[1]. But this type of methods suffers from great computation cost. The famous FCLS algorithm is a most successful one^[2]. But it still needs plenty of iterations and high computation consuming, especially with more endmembers. In order to make the iteration less and speed up computation of single iteration, many works has been done in

the field. Ren^[3] prompted a modified FCLS, replacing the original expressions for constraints by new ones. Wang^[4] prompted a pattern of distance computation and a way of determining unmixing endmembers, performs better than FCLS with less endmembers. Yang^[5] estimates abundance with ratio of simplex volume and projects the mixed pixel onto valid hyperplane, so as to acquire abundance fully constrained quickly. It also achieves better results when the number of endmembers is not so large.

Here in this paper, an algorithm based on orthogonal vector projection is proposed. Both the unconstrained abundances estimation and the valid endmembers determination are executed under the same principle of orthogonal vector projection. Firstly, several geometric methods for abundance estimation are introduced in the second part. Secondly, different ways of geometry procession promising fully constraints are listed. The prompted method is also illustrated then. At last, experiments results on these algorithms are given. They are compared in time and error points of view. Conclusions are provided at the end.

2. Geometric methods for estimating abundance

In order to speed up estimation of unconstrained abundance, geometric methods are preferred much in past years. Geng^[4] compute volumes ratio between the simplex of endmember set with one endmember being replaced by the mixed pixel and that of the original endmember set, which is viewed as the abundance of the replaced endmember in the mixed pixel. Luo^[4] use the distance ratio instead of volume ratio, so that it has better time performance than Geng. Wang^[4] gives a distance function for each pixel, which saves a lot of time. And Yang^[5] uses Cramer's rule speed up volume computation. Here in this paper, we use the orthogonal vector projection to generate the abundance, which is proposed recently^[6].

Assume that there are p target signatures, $\mathbf{m}_1, \mathbf{m}_2, \dots, \mathbf{m}_p$, referred to as endmembers that can be used to form a linear mixing model and any data sample vector \mathbf{r} can be represented as a linear mixture of these endmembers.

$$\mathbf{r} = \mathbf{M}\mathbf{a} + \mathbf{n} \quad (1)$$

where \mathbf{a} is abundance vector, \mathbf{n} is noise or can be interpreted as a measurement or model error.

Suppose that there is a set of orthogonal base $\tilde{\mathbf{m}}_1, \tilde{\mathbf{m}}_2, \dots, \tilde{\mathbf{m}}_p$ corresponding to the original signature vectors $\mathbf{m}_1, \mathbf{m}_2, \dots, \mathbf{m}_p$, detection fraction of \mathbf{m}_p in vector \mathbf{r} can be obtained as

$$\hat{\alpha}_p^{\text{OVP}}(\mathbf{r}) = \tilde{\mathbf{m}}_p^T \mathbf{r} \quad (2)$$

$\hat{\alpha}_p^{\text{OVP}}(\mathbf{r})$ can also be derived as a least squares OVP (LSOVP) to estimate α_p , denoted by $\hat{\alpha}_p^{\text{LSOVP}}(\mathbf{r})$ as

$$\hat{\alpha}_p^{\text{LSOVP}}(\mathbf{r}) = (\tilde{\mathbf{m}}_p^T \tilde{\mathbf{m}}_p)^{-1} \tilde{\mathbf{m}}_p^T \mathbf{r} = \hat{\alpha}_p^{\text{OVP}}(\mathbf{r}) / \|\tilde{\mathbf{m}}_p\|^2 \quad (3)$$

The well-known Gram Schmidt orthogonalization process (GSOP) can be used to orthogonalize all endmembers to remove the dependency of 2nd order statistics among all the endmembers in the same way as P_U^\perp does in OSP. By taking advantage of GSOP there is no need of inverting any matrix. But only inner products are required.

OVP Via Gram Schmidt Orthogonalization Process

(1) Initial condition: $\tilde{\mathbf{m}}_1 = \mathbf{m}_1$

(2) At j th target \mathbf{m}_j find $\tilde{\mathbf{m}}_j$ orthogonal to the space linearly spanned by $\tilde{\mathbf{m}}_1, \tilde{\mathbf{m}}_2, \dots, \tilde{\mathbf{m}}_{j-1}$ by

$$\tilde{\mathbf{m}}_j = \mathbf{m}_j - \sum_{i=1}^{j-1} \frac{\mathbf{m}_j^T \tilde{\mathbf{m}}_i}{\tilde{\mathbf{m}}_i^T \tilde{\mathbf{m}}_i} \tilde{\mathbf{m}}_i \quad (4)$$

- (3) Check if $j = p$. If yes, go to step 4. Otherwise, let $j \leftarrow j + 1$ and go to step 2.
(4) The OVP and LSOVP abundance fraction of α_p can be computed by (2) and (3).

3. Geometry based fully constrained estimation

As mentioned above, the resulted vector $\tilde{\mathbf{m}}_p$ after Gram-Schmidt orthogonal processing is actually the residual vector of \mathbf{m}_p after being projected onto space spanned by other endmembers. It provides the direction and height of the vertex corresponding to the p th endmember in the simplex formed by all endmembers. Any pixel vector \mathbf{r} whose value is negative or greater than 1 when being projected on to $\tilde{\mathbf{m}}_p$ means that it locates outside of the simplex, and its abundance will not satisfy sum-to-one and nonnegative. What we can do is to modify the pixel in the opposite direction $\tilde{\mathbf{m}}_p$ with the exceeded length, until it falls into the simplex. With this operation, we can prompt a new algorithm realizing fully constrained unmixing to accomplish the same thing with fully constrained Least Square (FCLS) method, which is called fully constrained orthogonal vector projection (FCOVP).

Given the endmember matrix $\mathbf{M} = [\mathbf{m}_1, \mathbf{m}_2, \dots, \mathbf{m}_p]$ and pixel $\mathbf{r} = [r_1, r_2, \dots, r_L]^T$, FCOVP can be described as follows.

- (1) Define $\mathbf{N} = \begin{bmatrix} \mathbf{M} \\ \mathbf{1} \end{bmatrix} = \begin{bmatrix} \mathbf{m}_1 & \mathbf{m}_2 & \dots & \mathbf{m}_p \\ 1 & 1 & 1 & 1 \end{bmatrix} = [\mathbf{n}_1, \mathbf{n}_2, \dots, \mathbf{n}_p]$, and $\mathbf{s} = [r_1, r_2, \dots, r_L, 1]^T$.
- (2) Compute $\tilde{\mathbf{n}}_1, \tilde{\mathbf{n}}_2, \dots, \tilde{\mathbf{n}}_p$ with each \mathbf{n}_i as the desired endmember. Project \mathbf{s} to each $\tilde{\mathbf{n}}_i$, $1 \leq i \leq p$, and the resulted projection vectors are p_1, p_2, \dots, p_p . If there is any $\mathbf{p}_i^T \tilde{\mathbf{n}}_i < 0$, define a deleting matrix $\mathbf{D} = \phi$ and go to step 3. Otherwise, go to step 9.
- (3) Pick up all the dissatisfy $\mathbf{p}_i^T \tilde{\mathbf{n}}_i < 0$, and take $\mathbf{p}_i' = -\mathbf{p}_i$ to form a new matrix \mathbf{P} .
- (4) Compute inner products of all vectors in \mathbf{P} , and form a projection ration matrix \mathbf{X} , $x_{kl} = \mathbf{p}_k'^T \mathbf{p}_l' (\mathbf{p}_k'^T \mathbf{p}_k')^{-1}$.
- (5) If all entries of \mathbf{X} are less than 1, move all original endmembers corresponding to vectors in \mathbf{P} into \mathbf{D} , and go to step 8.
- (6) If there are entries x_{kl} equals to or greater than 1, move endmembers corresponding to \mathbf{p}_l' into \mathbf{D} .
- (7) If there are entries x_{kl} less than 0, move endmembers corresponding to \mathbf{p}_k' and \mathbf{p}_l' into \mathbf{D} .
- (8) Delete all vectors in \mathbf{D} from \mathbf{N} , resulting into matrix \mathbf{N}' . Project \mathbf{s} onto space spanned by \mathbf{N}' , and let $\mathbf{s} \leftarrow \mathbf{P}_{\mathbf{N}'} \mathbf{s}$. Project \mathbf{s} to $\tilde{\mathbf{n}}_1, \tilde{\mathbf{n}}_2, \dots, \tilde{\mathbf{n}}_p$ to obtain the projection vectors p_1, p_2, \dots, p_p . If for all $1 \leq i \leq p$ $\mathbf{p}_i^T \tilde{\mathbf{n}}_i \geq 0$, go to step 9. Otherwise, go to step 3.
- (9) Compute the abundance vector $\boldsymbol{\alpha}^{FCOVP} = (\alpha_1, \alpha_2, \dots, \alpha_p)$, where $\alpha_i = p_i^T \tilde{\mathbf{n}}_i / (\tilde{\mathbf{n}}_i^T \tilde{\mathbf{n}}_i)$.

4. Experiments

The image scene shown in Fig. 1 was acquired by the airborne Hyperspectral Digital Imagery Collection Experiment (HYDICE) sensor in August 1995 from a flight altitude of 10000 ft with ground sampling distance approximately 1.5 m.

It has 210 spectral channels ranging from 0.4 μm to 2.5 μm with spectral resolution is 10 nm. The low signal/high noise bands: bands 1-3 and bands 202-210; and water vapor absorption bands: bands

101-112 and bands 137-153, were removed. So, a total of 169 bands were used for the experiments. It has size of 64×64 pixel vectors shown in Each element in Fig. 1 is a square panel and denoted by p_{ij} with rows indexed by $i = 1, 2, \dots, 5$ and columns indexed by $j = 1, 2, 3$. The 1.56m-spatial resolution of the image scene suggests that most of the 15 panels are one pixel in size except that the panels in the 1st column with the 2nd, 3rd, 4th, 5th rows which are two-pixel panels, denoted by p_{211} , p_{221} , p_{311} , p_{312} , p_{411} , p_{412} , p_{511} , p_{521} . As a result, there are a total 19 panel pixels. Figure 1 shows the precise spatial locations of these 19 panel pixels where red pixels (R pixels) are the panel center pixels and the pixels in yellow (Y pixels) are panel pixels mixed with the background.

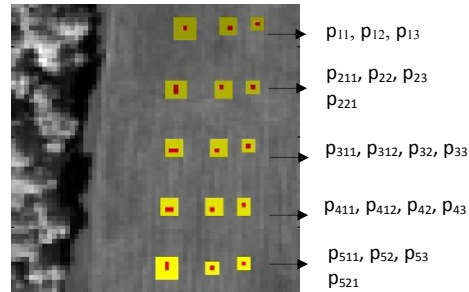


Figure 1. HYDICE image scene

The endmembers are generated by ATGP, used in the following experiments. Firstly, Wang^[4], Yang^[5], FCLS^[2] and the prompted algorithm(FCOVP) are compared according to time cost when they are applied on selected data from the Hydice image, shown in figure 2 and table 1.

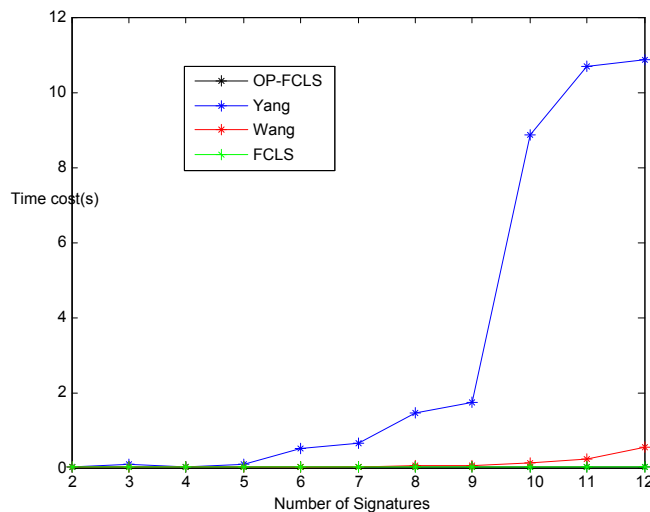


Figure 2. Time comparison between 4 algorithms on mixed pixels.

Tab.1 Time costs of 4 algorithms on mixed pixels

Number of Signatures	FCOVP	Yang	Wang	FCLS
2	0.031564	0.004385	0.003216	0.004158
3	0.004598	0.095991	0.002723	0.005106
4	0.007413	0.014343	0.004144	0.006352
5	0.007356	0.075013	0.009035	0.009505
6	0.010112	0.507734	0.018116	0.012804
7	0.012564	0.653355	0.025525	0.017032
8	0.013378	1.440667	0.042037	0.022518
9	0.012671	1.726858	0.063594	0.020226
10	0.016409	8.876636	0.120782	0.023103
11	0.020771	10.691623	0.237701	0.026382
12	0.018315	10.842767	0.550031	0.029665

From figure 2 and table 1, it can be found that FCOVP has a good time performance. Wang is faster than FCLS with less signatures, but it grows greatly when the number is bigger. Yang is the slowest one with the test pixels. As for the unmixing error, these four algorithms' performances are shown in table 2.

Tab.2 Unmixing error of 4 algorithms on mixed pixels

Number of Signatures	FCOVP	Yang	Wang	FCLS
2	17558.218	17546.027	17560.929	17560.929
3	17352.010	17348.807	17363.544	17363.544
4	1798.735	1797.265	1797.351	1797.351
5	1911.508	1797.145	1797.234	1797.234
6	1909.904	1795.534	1795.345	1795.345
7	1367.382	1367.370	1367.254	1367.255
8	1365.142	1365.129	1365.201	1365.166
9	695.708	695.691	695.724	695.724
10	694.417	694.461	694.431	694.432
11	661.847	661.826	661.863	661.863
12	647.250	647.229	647.263	647.263

From table 2, the unmixing error of Wang and FCLS is bigger than the other two algorithms. And Yang has the best performance. Because all algorithms are optimizing process, there is no one get the optimal solution actually. That means the results are just different sub-optimal solutions. Therefore, if the test data change, the compared results will change accordingly.

5. Conclusions

All the algorithms here are optimizing versions to solve the fully constraints problem. Different ways of optimization will achieve different results and performances when test data changes. The traditional FCLS often has a better performance with more signatures. But when the number is small, Wang and the FCOVP both have better performance. As for the unmixing error, it's hard to tell which one is the best because none of them is optimal. But it is sure that the orthogonal projection based methods do not make it worse, and for some data they are better. The detailed features of these algorithms need to be analyzed deeply later, which is believed more valuable.

Acknowledgment

This work was supported by the Fundamental Research Funds for the Central Universities under grant 3132015045.

References

- [1] J. J. Settle and N. A. Drake, "Linear mixing and estimation of groundcover proportions," *Int. J. Remote Sens.*, 14(6), 1159–1177 (1993)
- [2] D. Heinz, C.-I. Chang, and M. L. G. Althouse, "Fully constrained leastsquares-based linear unmixing," *Proc. Int. Geosci. Remote Sens. Symp.*, 1401–1403 (1999)
- [3] C.-I. Chang, *Hyperspectral Data Processing: Signal Processing Algorithm Design and Analysis*. Wiley, N.J., (2013)
- [4] L. Wang, D. Liu and Q. Wang, "Geometric Method of Fully Constrained Least squares Linear Spectral Mixture Analysis," *IEEE Transactions on Geoscience and Remote Sensing*, 51(6), 3558–3566 (2013)
- [5] H. Yang, J. An and C. Zhu, "Subspace-Projection-Based Geometric Unmixing for Material Quantification in Hyperspectral Imagery," *IEEE Journal of Selected Topics in Applied Earth Observations and Remote Sensing*, 7(6), 1966–1975 (2014)
- [6] M. Song, H.-C. Li, C.-I. Chang and Y. Li, "Gram-Schmidt Orthogonal Vector Projection for Hyperspectral Unmixing," *Proc. IGARSS*, 2934 – 2937 (2014)